



**HAL**  
open science

## Assessment of the Evolution of Temporal Segmental Strain in a Longitudinal Study of Myocardial Infarction

Bianca Freytag, Nicolas Duchateau, Lorena Petrusca, Jacques Ohayon, P Croisille, Patrick Clarysse

► **To cite this version:**

Bianca Freytag, Nicolas Duchateau, Lorena Petrusca, Jacques Ohayon, P Croisille, et al.. Assessment of the Evolution of Temporal Segmental Strain in a Longitudinal Study of Myocardial Infarction. 12th International Conference on Functional Imaging and Modeling of the Heart (FIMH 2023), LNCS, Jun 2023, Lyon, France. pp.678-687. hal-04096727

**HAL Id: hal-04096727**



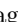



**<https://hal.science/hal-04096727>**

Submitted on 13 May 2023

**HAL** is a multi-disciplinary open access archive for the deposit and dissemination of scientific research documents, whether they are published or not. The documents may come from teaching and research institutions in France or abroad, or from public or private research centers.

L'archive ouverte pluridisciplinaire **HAL**, est destinée au dépôt et à la diffusion de documents scientifiques de niveau recherche, publiés ou non, émanant des établissements d'enseignement et de recherche français ou étrangers, des laboratoires publics ou privés.

# Assessment of the Evolution of Temporal Segmental Strain in a Longitudinal Study of Myocardial Infarction

Bianca Freytag<sup>1</sup> , Nicolas Duchateau<sup>2,3</sup> , Lorena Petrusca<sup>2,4</sup> , Jacques Ohayon<sup>1,5,6</sup> , Pierre Croisille<sup>2,4</sup> , and Patrick Clarysse<sup>2</sup> 

<sup>1</sup> Univ. Grenoble Alpes, CNRS, TIMC UMR 5525, Grenoble, France

[bianca.freytag@univ-grenoble-alpes.fr](mailto:bianca.freytag@univ-grenoble-alpes.fr)

<sup>2</sup> Univ. Lyon, INSA-Lyon, Université Claude Bernard Lyon 1, CNRS, Inserm, CREATIS UMR 5220, U1294, Lyon, France

<sup>3</sup> Institut Universitaire de France (IUF), Paris, France

<sup>4</sup> Department of Radiology, Hôpital Nord, Univ. Hospital of Saint-Étienne, France

<sup>5</sup> Center for Cardiovascular Regeneration, Department of Cardiovascular Sciences, Houston Methodist Research Institute, Houston, TX, USA

<sup>6</sup> Savoie Mont-Blanc Univ., Polytech Annecy-Chambéry, Le Bourget du Lac, France

**Abstract.** In this study, we propose an approach for the assessment of the evolution of heart function in a population of ST-elevation myocardial infarction (STEMI) patients. The patients were imaged using cine MRI with late gadolinium enhancement at 1 month after STEMI and at follow-up 12 months later. We reduced the dimensionality of the temporal strain data in order to represent the segmental strain patterns found in these individuals in a more compact manner. Then, this compact description of strain was used to identify left ventricular segments with abnormal function, as compared to a control group of healthy patients, and to investigate if 1) the compact representation of the patterns is more effective in predicting scarring than traditional measurements; and 2) how the strain patterns evolve over the following months. To that end, we offer a method for tracking strain evolution and, in particular, comparing infarcted regions with remote regions and healthy hearts. On a population of 29 STEMI patients and 18 controls, we found that, despite considering the extent of the lesion, we were not able to identify a clear mechanism of evolution; nonetheless, the technique may be beneficial in subsequent, larger longitudinal studies to quantitatively characterise patient outcomes.

**Keywords:** Temporal strain · Myocardial Infarction · Dimensionality Reduction · Abnormality Quantification

## 1 Introduction

Feature tracking based on routinely collected non-contrast cine magnetic resonance imaging (MRI) sequences may quantify myocardial deformation during

cardiac contraction [5,6]. Myocyte necrosis and subsequent scarring following myocardial infarction alter the mechanical characteristics of the myocardium, resulting in altered global and segmental strain [15]. Chronic myocardial scars, in particular those with wall thinning and obvious wall motion abnormalities, cause severe segmental strain impairment, which may be exploited to discriminate scar tissue from remote myocardium [14].

Late gadolinium enhancement (LGE) identifies infarcted myocardium in vivo, where myocardial contractility is unlikely to be restored during coronary revascularization [7]. However, the use of the contrast agent gadolinium poses a risk to patients with severe renal impairment [13]. As a result, it is desirable to accompany and eventually replace LGE images with other means, such as strain information derived from feature tracking in cine imaging [16].

The formation of scars in the myocardium after ST-elevation myocardial infarction (STEMI) can occur within a few days as the acute phase of the infarction resolves and the tissue begins to heal. The transition from acute to sub-acute infarction typically occurs within the first 2–3 weeks after the initial injury [12]. However, the healing process can continue for several months, and factors such as the size of the infarct, the patient’s age and overall health, and the presence of comorbidities can all impact the rate of healing.

The consequence of scarring on segmental strain over time is rarely investigated. A few studies looked at segmental myocardial strain as a predictor of cardiac function and mortality over longer time periods (such as one year) [1,2,9]. These studies used echocardiography, which is highly dependent on image quality and inconsistent in accuracy and reproducibility, specifically when measuring segmental strains [10]. Furthermore, *Mollema et al.* [9] and *Antoni et al.* [2] used a semi-quantitative wall motion score index and peak strains rather than the full temporal strain curves. Only *Mollema et al.* and *Abate et al.* [1] compared changes in basic strain measurements at follow-up. Another group compared strain in acute versus sub-acute infarcts (4–5 weeks after STEMI) assessed by MRI, which may be too short to see remodelling because of still ongoing pathophysiological processes [11].

In this study, the changes in segmental, temporal strain patterns from non-contrast cine images were analysed in patients 1 and 12 months after STEMI. The primary focus was on the changes in these patterns between the two visits, but the study also investigated whether using a compact representation of the patterns is more effective than traditional measurements, such as peak strains.

## 2 Methods

### 2.1 Experimental Data

This study investigated left ventricular (LV) strain in two cohorts.

The first dataset was a sub-group of the HIBISCUS-STEMI cohort, for which STEMI patients, treated with primary percutaneous coronary intervention in the cardiac intensive care unit of the Hospices Civils de Lyon, France, were

**Table 1.** Demographic data (mean  $\pm$  standard deviation). BSA: Body surface area. LVM: left ventricular mass. EDV: end-diastolic volume. ESV: end-systolic volume. EF: ejection fraction. A p-value  $\geq 0.05$  was considered not significant (NS).

	Control	STEMI	P-value (t-test)
N (N male)	18 (13)	29 (25)	
Age (years)	52.9 $\pm$ 16.0	56.3 $\pm$ 8.8	NS
BSA (m <sup>2</sup> )	1.91 $\pm$ 0.18	1.91 $\pm$ 0.19	NS
LVM (g)	95.5 $\pm$ 24.9	106.9 $\pm$ 26.8	NS
EDV (ml)	142.9 $\pm$ 28.3	165.6 $\pm$ 42.1	< 0.05
ESV (ml)	59.9 $\pm$ 15.9	86.6 $\pm$ 37.9	< 0.01
EF (%)	58.4 $\pm$ 6.2	49.5 $\pm$ 10.9	< 0.01

prospectively enrolled. Patients underwent cardiac MRI 1 month and 12 months after their admission for STEMI. 2-chamber, 4-chamber, and ventricular short-axis cine images, as well as LGE images, were acquired. Further details can be found in [3]. 29 patients with infarcts in the left anterior descending (LAD) artery were selected, while patients with infarcts in other territories were excluded.

The second dataset, the control group, consisted of 18 subjects and was part of the MARVEL cohort. These participants were healthy, sedentary volunteers of various ages. They were also scanned following the same protocol as above.

The demographics of both groups are listed in Table 1. The two groups were similar in age, body surface area, and LV mass. The gender proportions were matched as closely as the base cohorts allowed. Both studies were approved by the local ethics committee and are registered at ClinicalTrials.gov (NCT03064503 and NCT03070496). All patients provided written, informed consent.

## 2.2 Calculation of Strain and LGE Extent

In both studies, LV segmentation was performed using the CVI42 software (Circle Cardiovascular Imaging, Calgary, Canada) on short-axis, 2-chamber, and 4-chamber long-axis images. LV mass, ejection fraction (EF), and cardiac index were calculated from this segmentation. The software’s Feature Tracking module was used to estimate circumferential, radial, and longitudinal strains and strain rates over the epicardial and endocardial surfaces throughout the cardiac cycle. Strains were calculated using the short-axis images and the 2- and 4-chamber long-axis views with respect to the end-diastolic configuration. End-diastole was defined to co-occur with the frame of the largest LV volume, and the strain curves were temporally aligned such that they all started at end-diastole with 0% strain. Longitudinal strain curves were found to be of poor quality or lacking coverage over some segments, so they were disregarded in further analysis. The strains and strain rates were exported on a per-segment basis, using 16 of the 17 AHA segments (excluding the apical segment). In addition, peak strains in circumferential and radial directions were also exported, as were wall thickening and end-diastolic wall thickness. CVI42 defines the frame with the smallest LV

**Table 2.** List of all calculated features, detailing the step in which they were calculated and if they had a high loading in the component loadings of the embedding PCA.

Calculated in	Feature	High loading in 2D embedding
PCA	PCs of circ./radial strains	1st and 2nd PCs
	PCs of circ./radial strain rates	no
CVI42	Ejection fraction	yes
	Cardiac Index	no
	Wall thickening	yes
	End-diastolic wall thickness	no
	Peak circ./radial strain	Radial peak strain only
	Time delay of peak circ./radial strain	no
	Percentage of LGE enhanced segment area	not incl. in embedding

volume as the frame at which end-systole occurs. This timepoint was confirmed by visually checking for maximum LV contraction. A time delay was calculated for each segment’s strain curve that signifies how much earlier or later the peak value for this strain curve was reached in comparison to end-systole.

In the STEMI group, infarcts were semi-automatically segmented from the LGE images using CVI42’s Tissue Characterization Module with a full-width at half maximum algorithm and guided by previous segmentation results [4]. Infarct size was assessed on a segment basis as a percentage of the segment area and written out for each of the 16 AHA segments.

### 2.3 Dimensionality Reduction of Temporal Strain Data

To reduce the dimensionality of the temporal strain data, a Principal Component Analysis (PCA) was applied to the circumferential and radial strains and strain rates individually. This approach allowed for the compact description and comparison of the major temporal patterns and has been shown to be useful for the identification of LV segments with abnormal function [14].

First, the PCA was fitted to the cases in the control group to establish the baseline patterns seen in a healthy population. Then, the fitted PCA was used to transform the control and STEMI strain and strain rate curves into their respective latent spaces. The number of components was chosen such that 95% of the variance was captured (5 principal components for circumferential strain, 4 for radial strain, and 11 and 12 for circumferential and radial strain rates, respectively).

The fitting of the PCA and any further steps were implemented in Python using the scikit-learn library.

### 2.4 Embedding of Strain Patterns to Visualise Evolution

As the number of features (9 and 23 latent dimensions for strain and strain rates, respectively, plus functional measurements as listed in Table 2) was too large to facilitate a simple, intuitive observation of the changes in strain patterns, a second PCA was fitted to the set of features to produce a 2-dimensional

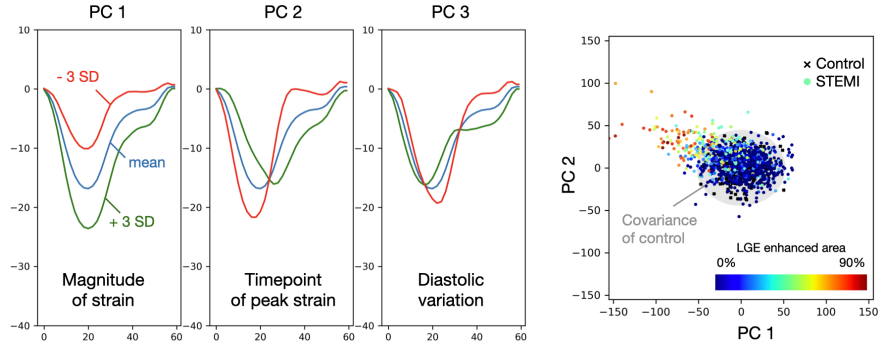


**Fig. 1.** Result of the PCA for circumferential strain. On the left, the first three principal components, fitted to the control group, are shown. On the right, each segment is represented by its first two principal components and colour-coded with the percentage of enhanced area for this segment (STEMI group). The majority of segments with an LGE enhanced area  $> 50\%$  lie outside the distribution of control cases as defined by the covariance of the control group.

embedding. This second PCA will further be called the “embedding PCA” to avoid confusion with the first PCA, which reduced the temporal strain curves to the strain patterns.

In a first step, all features were averaged over the LAD territory (AHA segments 1, 2, 7, 8, 13, 14) and the remaining “remote” segments. Then, the embedding PCA was fitted to both the control and the STEMI groups to create the two-dimensional map shown in Fig. 2. The last step consisted of the calculation of 1) the Euclidean distance between the two samples representing the strain at months 1 and 12 for the LAD territory and remote regions of each individual heart in the 2D embedding plane, and 2) the Mahalanobis distance of each sample with respect to the control group distribution.

### 3 Results

The results of the first PCA, which reduced the temporal strain curves to strain patterns, were well aligned with previous findings by *Tabassian et al.* [14]. Cardiac strain in infarcted segments was hypothesised to be 1) smaller in amplitude (hypokinetic) or even dyskinetic (positive strain where negative was expected and vice versa) and 2) dyssynchronous (variations in timing of shortening and lengthening of the segments) [15]. These patterns were reflected in the first and second principal components in both radial and circumferential strain, as illustrated in Fig. 1. When applying the condition that 95% of the variance should be explained by the principal components, the number of components needed to be increased to more than 10 for the two strain rates, but when looking at their

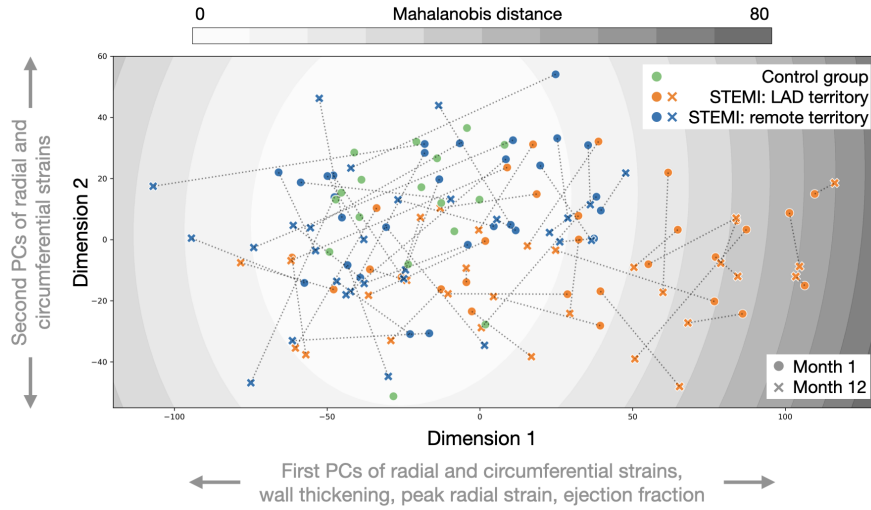


**Fig. 2.** Two-dimensional embedding of strain patterns in LAD, remote, and control segments. For the STEMI group, the evolution in strain features is represented by dashed lines between months 1 and 12. The Mahalanobis distance with respect to the control group is indicated by the grey contours. The features that vary strongly in the two dimensions are listed along the axes.

importance for the component loadings of the embedding PCA, all were deemed to have little variation in the dimensions of the embedding PCA.

Previous studies have attempted to detect the presence of infarcts with a single, strain-related (global, not segmental) value [8], but in the present study, there was no individual feature and no small number of combined features, calculated in the primary PCA, that correlated highly with the extent of LGE.

With two extracted dimensions, the embedding PCA covered 93.5% of the variance in the features. The embedding PCA component loadings showed that dimension 1 (which explained 78.2% of variance) best explained the variance in the first principal components of radial and circumferential strain, wall thickening, peak radial strain, and ejection fraction, while the second principal components of radial and circumferential strain varied most along the direction of dimension 2 (which explained 15.3% of variance). This meant that the two main temporal strain patterns (amplitude of strain and time delay of peak strain) were well encoded in the resulting 2-dimensional embedding. Interestingly, the two classic measurements, circumferential and radial peak strain, showed little variation in dimension 1 and only weak importance in dimension 2. The loading values for all of the other features listed in Table 2 were also low.

In Fig. 2, the resulting parameter space of the two embedding PCA dimensions is depicted. There was a group of segments belonging to the LAD territory that was outside of the main distribution consisting of control cases and remote

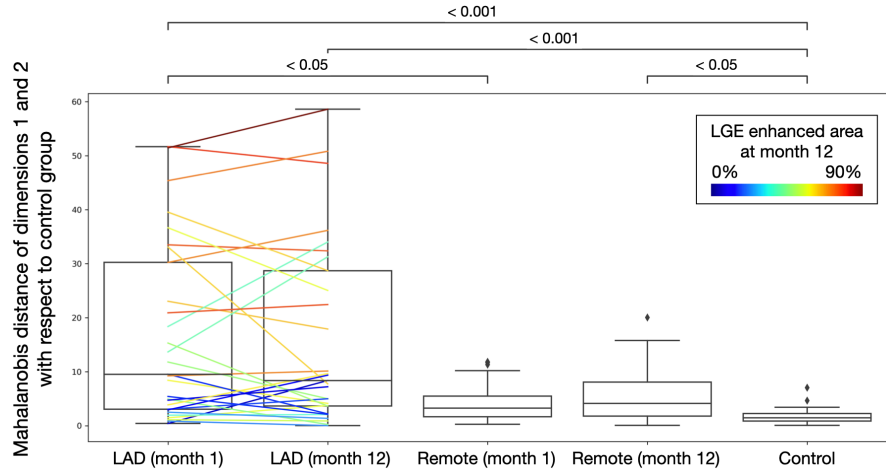


**Fig. 3.** Comparison of the Mahalanobis distance for the three regions at months 1 and 12. For the LAD (STEMI) territory, the evolution between the two timepoints of each segment in terms of the Mahalanobis distance is presented with a line, colour-coded by the percentage of LGE enhanced area at month 12. Higher LGE scores were associated with a greater Mahalanobis distance, but there was no evidence that the percentage of LGE had an effect on the direction of evolution.

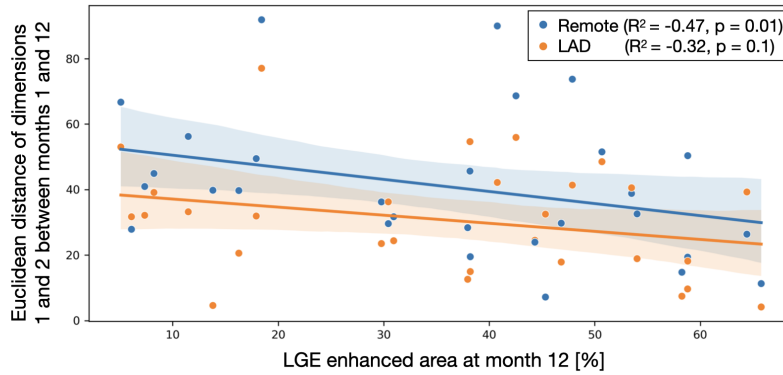
segments, but there was no clear clustering. The cases with high dimension 1 values coincided with the cases of high LGE, and the regression between dimension 1 and LGE has a correlation coefficient of  $R^2 = 0.75$  and a p-value of  $< 0.01$ .

Figure 3 shows the Mahalanobis distance of the LAD and remote segments versus the control group segments. The Mahalanobis distance in the segments within the LAD (STEMI) territory was significantly elevated in comparison to the control group segments. The plot allows one to look at the direction in which segments evolved, such as recovering towards the control group (negative slope) or evolving further away from the normal strain (positive slope). There was no clear direction of evolution, either when looking at cases of high or low percentages of LGE-enhanced area.

When considering the Euclidean distance between timepoints month 1 and month 12, remote segments tended to move more than infarcted segments (Fig. 4), and, overall, segments within hearts that had a high percentage of LGE enhanced area moved less than their counterparts in hearts with a low LGE score.

While dimension 1 of the embedding PCA correlated well with the amount of LGE ( $R^2 = 0.77$ ), the question remains if this complex indicator, which takes into account the strain patterns as well as some global functional measurements, is better than commonly used strain indicators of reduced cardiac contraction, such as peak strains. Indeed, peak circumferential strain ( $R^2 = 0.85$ ) and peak radial strain ( $R^2 = 0.8$ ) correlated well with LGE, too.





**Fig. 4.** Euclidean distance between months 1 and 12, representing the change each segment underwent in terms of strain.

## 4 Discussion

Infarcted segments in the LAD territory were thought to evolve differently than segments in the remote territory at the outset of the study. At month 1, the infarct can be considered stable and the inflammation resolved, so that the extent of the infarct and strains at month 12 remain unchanged. For the remote segments, their evolution was not as clear; one hypothesis was that in hearts with small infarcts, strain may change very little over time as the overall ability of the heart to contract is not much reduced. Vice versa, in hearts with severe infarcts, the remote segments may have to contract harder to generate sufficient cardiac output. In this paper, there was no evidence to support such hypotheses.

There was also no clear indication as to why segments evolved favourably or worsened in terms of strain. A few reasons for this, apart from the fact that such evolution may in fact not be reliably predicted by current measurements of strain, lie in the shortcomings of this study: 1) The size of the two groups was small; 2) only the LAD territory was considered; and 3) longitudinal strain was omitted for quality reasons but is commonly, at least as a global measurement, regarded as a good predictor of the presence of infarction. Further validation of the strain calculations, with the aim to include longitudinal strains, is needed to ensure that the inability to detect a clear evolution of cardiac dysfunction in STEMI patients is not due to inaccuracies with the overall strain calculations or the omission of longitudinal strain information.

In another paper that followed a very similar dimensionality reduction scheme, strain and strain rates were found to have higher predictive power for LGE [14] than classically used end-systolic strains. Interestingly, here, strain rates played an inferior role, and there was no single, individual feature or small number of combined features that correlated better with LGE than peak strains; this may be explained by the different imaging modality (echocardiography versus feature tracking from MRI) or calculation method. Only a few previous studies looked at

longitudinal datasets. *Polacin et al.* [11] found that cine sequences could detect 75–80% of infarcts and that some scarred segments were reclassified with respect to their LGE score, but they also did not note any significant changes between the two imaging timepoints, which were 3–12 weeks apart.

In the future, it would be very interesting to investigate the influence of the imaging timepoint on the observed evolution. The first imaging timepoint at month 1 was well into the recovery of the inflammation and remodelling following STEMI. Therefore, an imaging timepoint shortly after treatment for STEMI may uncover a more pronounced evolution in terms of strain and LGE.

## 5 Conclusion

This study is exploratory in that it aims to investigate the evolution of temporal, segmental strain in STEMI patients over a time period long enough to ensure concluded and stable remodelling. It employed the entire temporal strain curves of each AHA segment rather than a single (semi-quantitative) measurement of wall motion or peak strains, and it described these strains in a concise manner by relating the strain to the most important temporal patterns.

On the considered set of STEMI cases, there was no clear trend in the evolution of strains between the two timepoints. The study shows that, when maintaining the temporal information in strain patterns, no better predictive power of LGE extend was achieved compared to classic measurements like peak strains.

However, the proposed approach to tracking the evolution of strain across time may be used in other longitudinal studies to help clinicians better understand the patient’s outcome.

**Acknowledgements** The authors would like to thank Michel Ovize, Thomas Bochaton, and Nathan Mewton for sharing in-vivo data from the HIBISCUS cohort. We also thank Circle Cardiovascular Imaging (Calgary, Canada) for making the CVI42 software package available for research purposes. We acknowledge the support of the French Agence Nationale de la Recherche (ANR) under grants ANR-19-CE45-0020 (SIMR project), ANR-11-LABX-0063 (LABEX PRIMES of Univ. Lyon), and ANR-19-CE45-0005 (MIC-MAC project), and the Fédération Française de Cardiologie (MI-MIX project, Allocation René Foudon).

## References

1. Abate, E., Hoogslag, G.E., Antoni, M.L., Nucifora, G., Delgado, V., Holman, E.R., Schalij, M.J., Bax, J.J., Marsan, N.A.: Value of Three-Dimensional Speckle-Tracking Longitudinal Strain for Predicting Improvement of Left Ventricular Function After Acute Myocardial Infarction. *Am. J. Card.* **110**(7), 961–967 (2012)
2. Antoni, M.L., Mollema, S.A., Delgado, V., Atary, J.Z., Borleffs, C.J.W., Boersma, E., Holman, E.R., van der Wall, E.E., Schalij, M.J., Bax, J.J.: Prognostic importance of strain and strain rate after acute myocardial infarction. *Eur. Heart J.* **31**(13), 1640–1647 (2010)

3. Bernelin, H., Mewton, N., Si-Mohamed, S., Croisille, P., Rioufol, G., Bonnefoy-Cudraz, E., Douek, P., Dufay, N., Amaz, C., Jossan, C., Ovize, M., Bochaton, T.: Nephilysin levels at the acute phase of ST-elevation myocardial infarction. *Clin. Cardiol.* **42**(1), 32–38 (2019)
4. Bochaton, T., Leboube, S., Paccalet, A., Crola Da Silva, C., Buisson, M., Mewton, N., Amaz, C., Varillon, Y., Bonnefoy-Cudraz, E., Rioufol, G., Cho, T.H., Ovize, M., Bidaux, G., Nighoghossian, N., Mechtouff, L.: Impact of Age on Systemic Inflammatory Profile of Patients With ST-Segment–Elevation Myocardial Infarction and Acute Ischemic Stroke. *Stroke* **53**(7), 2249–2259 (2022)
5. Cao, J.J., Wang, Y., McLaughlin, J., Haag, E., Rhee, P., Passick, M., Toole, R., Cheng, J., Berke, A.D., Lachman, J., Reichel, N.: Left Ventricular Filling Pressure Assessment Using Left Atrial Transit Time by Cardiac Magnetic Resonance Imaging. *Circ. Cardiovasc. Imaging* **4**(2), 130–138 (2011)
6. Claus, P., Omar, A.M.S., Pedrizzetti, G., Sengupta, P.P., Nagel, E.: Tissue Tracking Technology for Assessing Cardiac Mechanics. *JACC Cardiovasc. Imaging* **8**(12), 1444–1460 (2015)
7. Kim, R.J., Rafael, A.R., Chen, E.L., Parker, M.A., Simonetti, O., Klocke, F.J., Bonow, R.O., Judd, R.M.: The Use of Contrast-Enhanced Magnetic Resonance Imaging to Identify Reversible Myocardial Dysfunction. *N. Engl. J. Med.* **343**(20), 1445–1453 (2000)
8. Mangion, K., McComb, C., Auger, D.A., Epstein, F.H., Berry, C.: Magnetic Resonance Imaging of Myocardial Strain After Acute ST-Segment–Elevation Myocardial Infarction: A Systematic Review. *Circ Cardiovasc Imaging* **10**(8) (2017)
9. Mollema, S.A., Delgado, V., Bertini, M., Antoni, M.L., Boersma, E., Holman, E.R., Stokkel, M.P., van der Wall, E.E., Schalij, M.J., Bax, J.J.: Viability Assessment With Global Left Ventricular Longitudinal Strain Predicts Recovery of Left Ventricular Function After Acute Myocardial Infarction. *Circ. Cardiovasc. Imaging* **3**(1), 15–23 (2010)
10. Pedrizzetti, G., Claus, P., Kilner, P.J., Nagel, E.: Principles of cardiovascular magnetic resonance feature tracking and echocardiographic speckle tracking for informed clinical use. *J. Cardiovasc. Magn. Reson.* **18**(1), 51 (2016)
11. Polacin, M., Karolyi, M., Eberhard, M., Matziris, I., Alkadhi, H., Kozerke, S., Manka, R.: Segmental strain for scar detection in acute myocardial infarcts and in follow-up exams using non-contrast CMR cine sequences. *BMC Cardiovasc. Disord.* **22**(1), 226 (2022)
12. Richardson, W.J., Clarke, S.A., Quinn, T.A., Holmes, J.W.: Physiological Implications of Myocardial Scar Structure. *Compr. Physiol.* **5**(4), 1877–1909 (2015)
13. Rogosnitzky, M., Branch, S.: Gadolinium-based contrast agent toxicity: A review of known and proposed mechanisms. *Biometals* **29**(3), 365–376 (2016)
14. Tabassian, M., Alessandrini, M., Herbots, L., Mirea, O., Pagourelas, E.D., Jassaityte, R., Engvall, J., De Marchi, L., Masetti, G., D’hooge, J.: Machine learning of the spatio-temporal characteristics of echocardiographic deformation curves for infarct classification. *Int. J. Cardiovasc. Imaging* **33**(8), 1159–1167 (2017)
15. Voigt, J.U., Cvijic, M.: 2- and 3-Dimensional Myocardial Strain in Cardiac Health and Disease. *JACC Cardiovasc. Imaging* **12**(9), 1849–1863 (2019)
16. Yu, S., Zhou, J., Yang, K., Chen, X., Zheng, Y., Zhao, K., Song, J., Ji, K., Zhou, P., Yan, H., Zhao, S.: Correlation of Myocardial Strain and Late Gadolinium Enhancement by Cardiac Magnetic Resonance After a First Anterior ST-Segment Elevation Myocardial Infarction. *Front. Cardiovasc. Med.* **8**, 705487 (2021)